Proceedings of the 8th U.S. National Conference on Earthquake Engineering
April 18-22, 2006, San Francisco, California, USA
Paper No. 1323

A SEMI-EMPIRICAL MODEL FOR THE ESTIMATION OF MAXIMUM HORIZONTAL DISPLACEMENT DUE TO LIQUEFACTION-INDUCED LATERAL SPREADING

Allison T. Faris[1], Raymond B. Seed[2], Robert E. Kayen[3], Jiaer Wu[4]

ABSTRACT

During the 1906 San Francisco Earthquake, liquefaction-induced lateral spreading and resultant ground displacements damaged bridges, buried utilities and lifelines, conventional structures, and other developed works. This paper presents an improved engineering tool for the prediction of maximum displacement due to liquefaction-induced lateral spreading. A semi-empirical approach is employed, combining mechanistic understanding and data from laboratory testing with data and lessons from full-scale earthquake field case histories. The principle of strain potential index, based primarily on correlation of cyclic simple shear laboratory testing results with in-situ Standard Penetration Test (SPT) results, is used as an index to characterize the deformation potential of soils after they liquefy. A Bayesian probabilistic approach is adopted for development of the final predictive model, in order to take fullest advantage of the data available and to deal with the inherent uncertainties intrinsic to the back-analyses of field case histories. A case history from the 1906 San Francisco Earthquake is utilized to demonstrate the ability of the resultant semi-empirical model to estimate maximum horizontal displacement due to liquefaction-induced lateral spreading.

Introduction

Liquefaction-induced lateral spreading, and resultant ground displacements and deformations, can be very damaging to bridges, buried utilities and lifelines, conventional structures, port and harbor facilities, and other developed works. In particular, disruption of water lines can reduce or eliminate the ability to fight (and extinguish) post-earthquake fires; this led to the disastrous post-earthquake fires that destroyed large portions of San Francisco in the wake of the 1906 San Francisco Earthquake.

[1] Engineer, Exponent, Inc., 5401 McConnell Ave, Los Angeles, CA 90066
[2] Professor, Dept of Civil and Environmental Engineering, University of California at Berkeley, Berkeley, CA 94720
[3] Civil Engineer, USGS, MS-999M, 345 Middlefield Road, Menlo Park, CA 94025
[4] Engineer, URS Corporation, 500 12th Street, Suite 200, Oakland, CA 94607

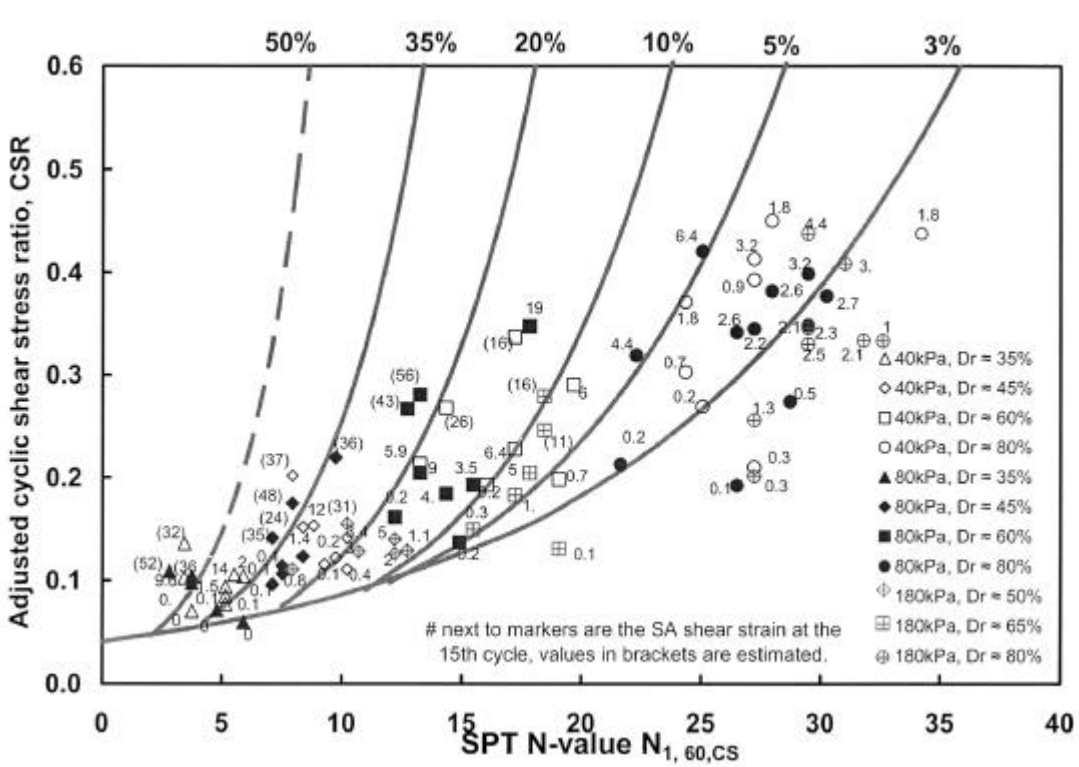

Figure 1. Relationship for Shear Strain Potential Index as a function of $N_{1,60,cs}$ and Equivalent Uniform Cyclic Stress Ratio, *CSR*, for M_w = 7.5 (Wu, 2002)

Background

Past efforts to estimate lateral displacement include: (1) empirical models, (2) analytical models, and (3) constitutive models. The empirical models are based solely on back analyses of field case histories of liquefaction-induced lateral spreading, largely without taking advantage of knowledge of the underlying mechanics of the phenomenon in development of the resulting empirical predictive tools. The exception to this is "semi-empirical" modeling, which gleans knowledge gained in laboratory testing programs to improve empirical efforts to model lateral spreading.

A semi-empirical approach is employed to develop an improved engineering tool for the prediction of maximum liquefaction-induced lateral spreading displacement, combining mechanistic understanding and data from laboratory testing with data and lessons from full-scale earthquake field case histories. A formally probabilistic approach is adopted for development of the final predictive model, in order to take fullest advantage of the data available and to deal with the inherent uncertainties intrinsic to the back-analyses of field case histories.

The principle of strain potential index, based primarily on correlation of cyclic simple shear laboratory testing results with in-situ Standard Penetration Test (SPT) results, is used as an index to characterize the deformation potential of soils after they liquefy (Wu, 2002). A lateral spread feature is considered to be a single case when a semi-coherent mass of soil displaced largely in a given direction. This differed from many previous studies, in which individual measured displacement vectors were treated as independent data points. Multiple displacement

vectors on the same spread feature were considered to be strongly correlated, and the overall feature was treated as one case.

In general, Displacement Potential Index, *DPI*, is calculated by estimating the Strain Potential Index, *SPI*, for each equivalent clean-sand corrected SPT blowcount, following the methodology of Seed et al (2001), in potentially liquefiable material. This shear strain potential is then applied to the sub-layer represented by individual blowcounts, resulting in a displacement potential for each sub-layer. Finally, *DPI* is calculated by cumulating the individual displacement potentials, from the bottom to the top of the boring.

The curves of shear strain potential developed by Wu (2002), shown in Fig. 1, are the basis of *DPI*. However, the laboratory data upon which the curves are based were generally taken to shear strain levels below 50 %, as limited by the laboratory testing devices. Therefore, the curves were slightly modified for application to the prediction of liquefaction-induced lateral spreading by the addition of a 75 % shear strain potential curve, as shown in Fig. 2. This curve was extrapolated judgmentally, using the surface described by the shear strain contours shown in Fig. 1 as a guide.

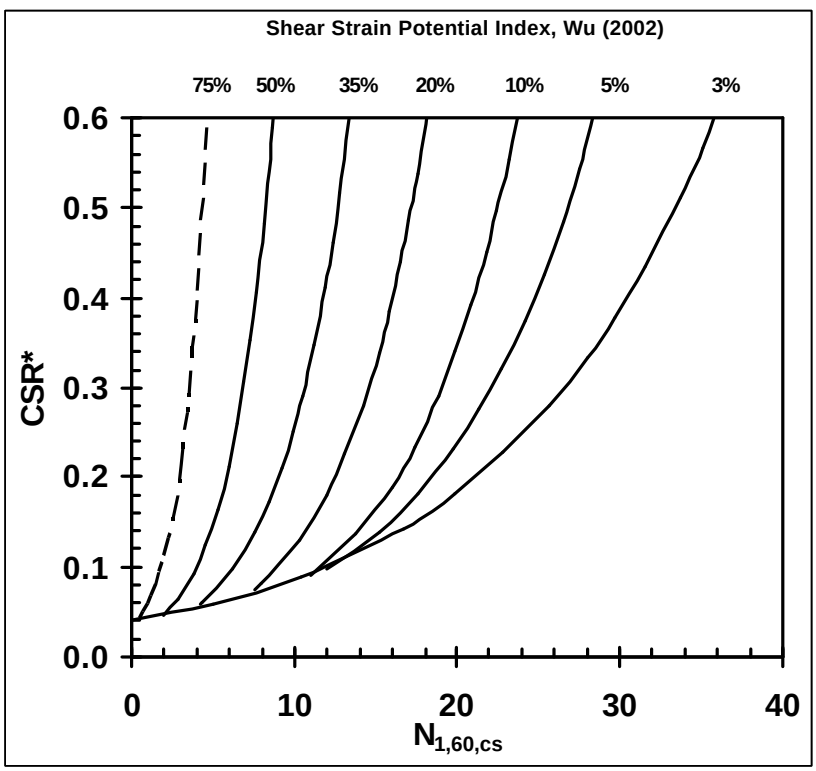

Figure 2. Modified Shear Strain Potential curves based on Wu (2002)

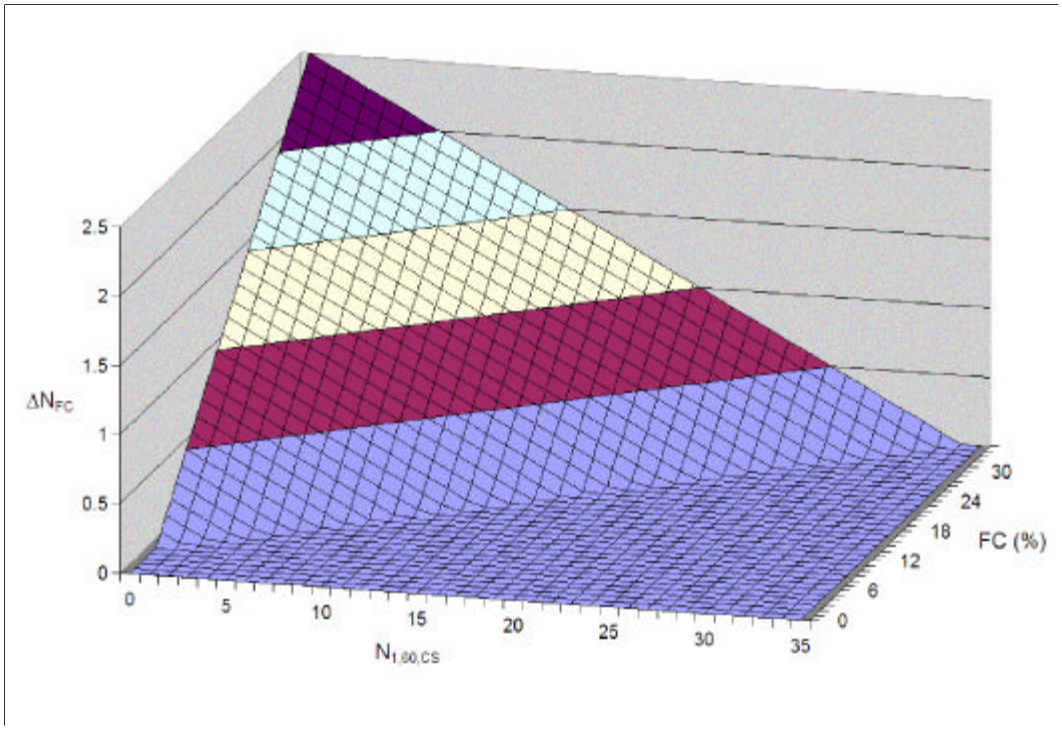

Figure 3. Fines content adjustment to modified Shear Strain Potential

Another restriction of the original laboratory data set was that most of the tests were performed on clean sand samples. Assessment of the field displacement data made it clear that this "clean sand" data overestimated displacements in silty soils with increasing fines content. Accordingly, an adjustment to the shear strain potential was necessary to accommodate the additional resistance to shear strain accumulation exhibited by materials with increasing fines content. The judgmentally-derived adjustment factor, ΔN_{FC}, is illustrated in Fig. 3. This results in a maximum increase of 2.5 blows/ft for very loose soils ($N_{1,60,cs}$ values near one) and high fines contents (FC = 35 %).

Case History Processing Procedure

A total of 45 lateral spread case histories were compiled and back-analyzed, from 14 earthquakes. Each case was first analyzed to determine which soil strata were likely to have liquefied. Next, the post-liquefaction global stability of each site was assessed. Four sites considered to be statically unstable were deleted from further consideration as they would experience "large", gravity-driven displacements until their geometry was rearranged sufficiently to reach a stable configuration. The remaining 41 cases were then analyzed, and strain potential indexes were calculated by summing liquefaction strain potential vertically through all strata at each location of an SPT boring.

Liquefaction Initiation Analysis Procedures

The probabilistic liquefaction initiation analysis procedure developed by Cetin (2000) and presented in Seed et al (2001) is performed for each boring at a site. To compliment this analysis, the deterministic NCEER-recommended procedure is also performed for each boring at a site (Youd et al, 2001). This is valuable because the influence of the variations in each procedure were

readily apparent (e.g. the influence of different nonlinear shear mass participation factors adopted by each procedure on the resulting in-situ cyclic shear stress ratio).

Post-Liquefaction Static Stability

After initial assessment of the likelihood of triggering of liquefaction, it is important to assess post-liquefaction static stability because the fundamental mechanics governing a "flow failure", i.e. a gravity-driven fluid-like mass movement, are different from liquefaction-induced lateral spreading, i.e. a shear stress influenced accumulation of strain distributed within liquefiable material. It is unreasonable to assume that a single model will accurately capture both phenomena. Simply put, this is the stage where the apples are separated from the oranges as gravity-driven flow "slumps" are separated from more stable cases which cyclically accumulate shear displacements during cyclic shaking. This was accomplished by performing limit equilibrium slope stability analyses of all free-face case histories.

Displacement Potential Index

The displacement potential index, *DPI*, described above, was calculated at the location of each boring within each liquefaction-induced lateral spread case history. It is important to note that potential shear strain, and hence potential displacement, was taken as zero for sub-layers that consisted of non-liquefiable soil types, e.g. high plasticity clays.

Characterization of Static Driving Shear Stress

The load due to gravity-induced static driving shear stresses is represented by α, the ratio of the horizontal driving shear stress to the vertical effective stress. This load is characterized, in these current studies, based on (1) the average slope of the ground surface (*S* in %) across the entire lateral spread feature, (2) the ratio of free-face height (*H* in m) to one quarter of the length (*L* in m) of the lateral spread, or (3) the addition of (1) and (2), if a site was characterized by both a free-face and sloping ground. This makes sense physically because these quantities represent proxies for the ratio of the average statically-induced horizontal shear stress, τ_{hv} , to the vertical effective stress, σ_v', the static equivalent of the cyclic shear stress ratio presented above. It is important to note that no distinction is made between the free-face and gently-sloping ground conditions, and that all combinations of free-face and sloping ground conditions are treated similarly.

Grading Criteria

Previous efforts at empirical modeling have been hampered by the dueling concerns of having enough data, in a statistical sense, while restricting a database to contain only high quality case histories. As a result, highly uncertain case histories have had undue influence on the final model parameters. In response to this dilemma, grading criteria were established and implemented in this work such that poor-quality case histories have correspondingly less influence on the regression of the model parameters, via an appropriate coefficient of variation. Fig. 4 shows all of the processed case histories, with error bars of plus/minus one standard deviation, which results from the grade each case is assigned. Based on this compilation of processed case histories, DPI_{max} shows promise as a predictor of the maximum horizontal displacement, H_{max} , measured within a lateral spread feature.

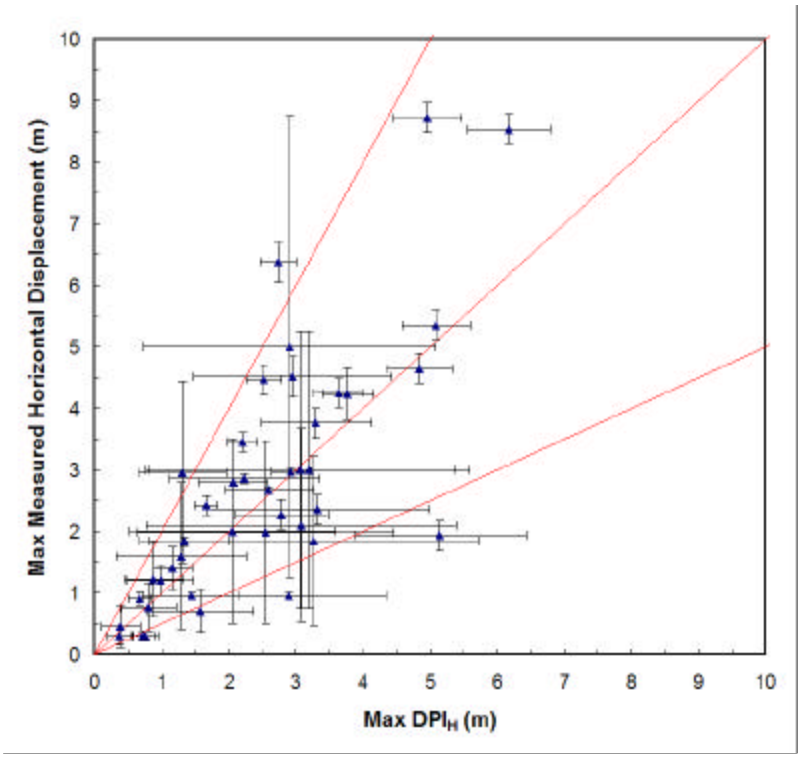

Figure 4. Comparison of maximum Displacement Potential Index, DPI_{max} , and maximum measured horizontal displacement, H_{max}

Semi-empirical model

Bayesian updating methods were implemented to accommodate the uncertainty that is present in a database of lateral spread case histories. An advantage of Bayesian methodology is the ability of the developer to apply judgment to the process. One example of this application of judgment in this research is the grading criteria, as mentioned previously.

Another example is the application of judgment during the selection of model parameters. As mentioned above, DPI_{max} appears to be a strong indicator of H_{max}. This is not surprising, as *DPI* is a compound factor representing a combination of a number of factors including: CSR_{eq}*, $N_{1,60,CS}$ and layer thickness, and cyclic loading intensity and duration. However, DPI_{max} is based on "level ground" cyclic simple shear tests and therefore does not reflect the influence of a static driving shear stress. The intention of this research is to reflect this influence with the addition of α, a parameter that is not case-dependent (i.e. free-face or sloping ground) and also that allows for a combination case (i.e. free-face and sloping ground).

Lastly, it is intuitive that duration of strong ground motion would influence the magnitude of lateral spread displacement, and consequently the maximum displacement. Often moment magnitude, M_w, is used as a proxy for duration, given that an increase in M_w often results in an increase in duration. While duration effects are implicitly included in the magnitude correction of cyclic shear stress ratio, CSR_{eq}*, which is an input into the calculation of potential displacement index, *DPI*, this magnitude-correlated duration adjustment of CSR_{eq} is based on a field case history data set for liquefaction initiation and not for lateral spreading. Therefore, M_w is included

as an additional model parameter to capture the additional influence of duration on the resulting maximum displacement.

Recommended Maximum Displacement Model

A number of mathematical predictive models were developed for the estimation of maximum horizontal displacement due to liquefaction-induced lateral spreading. The following model was among the simplest of these and provided results that were similar in accuracy to the more complex formulations while maintaining simplicity and ease of engineering use:

$$H_{max} = \theta_1 DPI_{max} + \theta_2 \alpha + \theta_3 M_w \qquad \text{(Equation 1)}$$

where H_{max} is the maximum horizontal displacement in meters; DPI_{max} is the maximum displacement potential index in meters; α represents the static load; M_w is the moment magnitude. θ_1 through θ_3 represent the regressed model parameters, based on use of Bayesian updating regression methods to regress the field case histories. It is intuitive that an increase in DPI_{max} , α , or M_w will increase the estimated displacement (H_{max}). Thus, θ_1, θ_2 and θ_3 are expected to have positive values. Alternative formulations included models that permitted nonlinearity in the relationship between H_{max} and (1) DPI_{max} , (2) α , and/or (3) M_w .

The final deterministic predictive equation, using mean values of the model parameters is presented as follows:

$$H_{max} = \exp(1.0443 \ln(DPI_{max}) + 0.0046 \ln(\alpha) + 0.0029 M_w) \qquad \text{(Equation 2)}$$

By using mean values of the model parameters, the predicted value is a point estimate of H_{max} and so does not consider the uncertainty in the model parameters. Fig. 5 compares the estimates of H_{max} to the maximum displacement measured at each lateral spread feature.

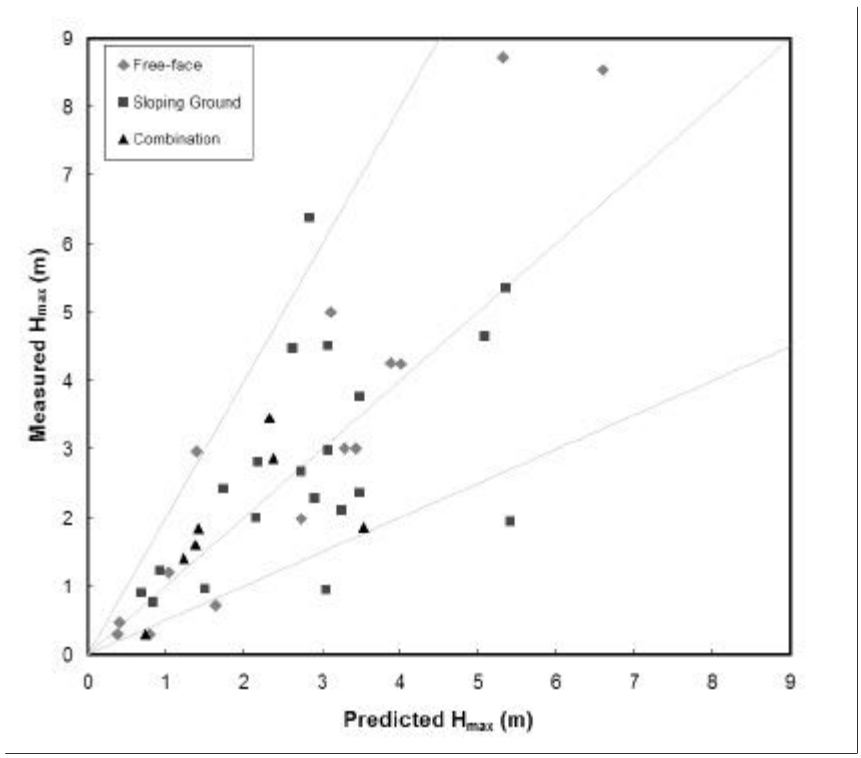

Figure 5. Model fit for the recommended semi-empirical correlation for prediction of maximum lateral spread displacement

Example Case History

Mission Creek Area

The Mission Creek area of San Francisco is located about 13 km from the fault rupture, on the western edge of San Francisco, as it had developed to that time within a former tidal creek and salt marsh (O' Rourke et al, 1992). The typical soil column at Mission Creek consists of 0-8 m of artificial fill overlying silty clay (Bay Mud). The artificial fill consists of loosely dumped debris and dune sand. The surficial effects of liquefaction fall within the lateral extent of the fill.

Soil borings were presented by O'Rourke et al. (1992). However, the blow counts were not SPT blowcounts because a larger sampler was used. Therefore, corrections for sampler size and energy imparted were estimated to convert these blowcounts to comparable SPT measurements (Bartlett, 1992). Liquefaction initiation analyses performed for the site, presented in Fig. 6, confirmed that loose sandy fill was likely to have liquefied during the event. The peak ground acceleration used for the analyses (0.37g) is estimated by averaging the attentuation relationships published in Abrahamson and Silva (1997) and Sadigh and Egan (1998). The shear wave velocity profile used for the r_d calculation at this site using Seed et al. (2001) was based on an average of three correlations between SPT blowcounts and shear wave velocity (Dickenson 1994, Seed et al 1984, and Sykora and Stokoe 1983).

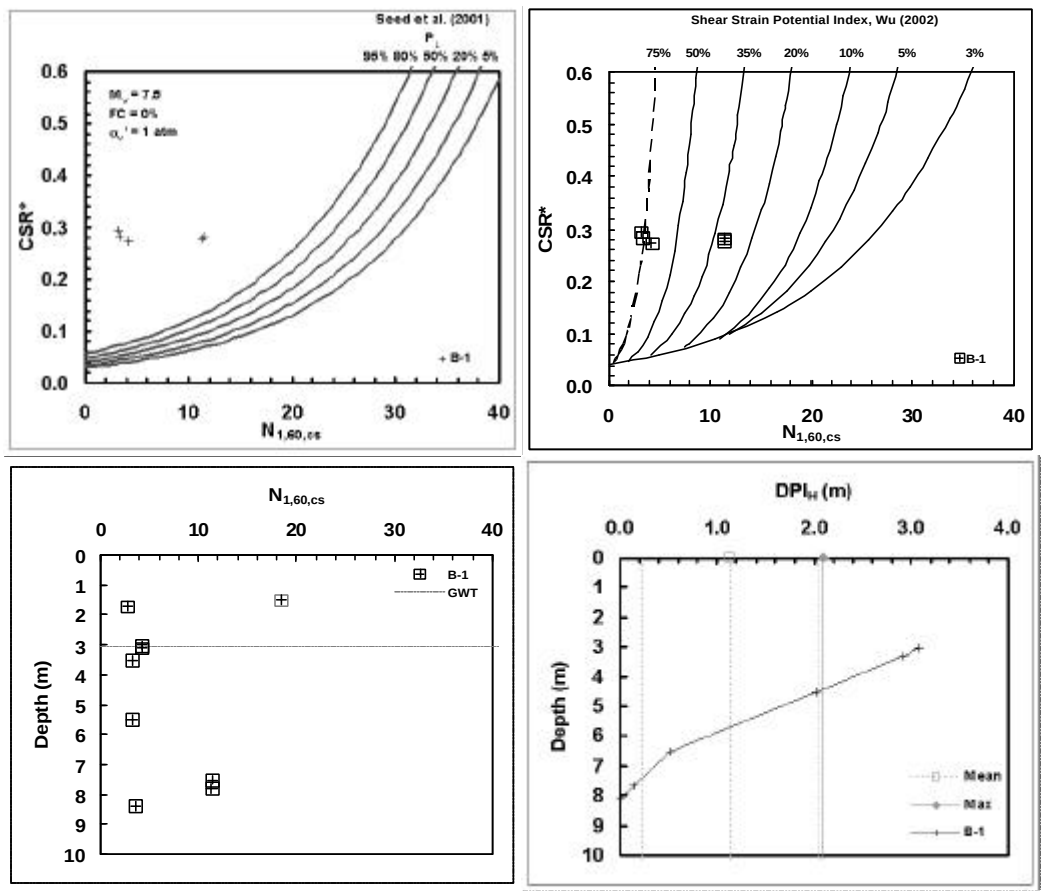

Figure 6. Results of liquefaction analyses at Mission Creek

The upper left plot in Fig. 6 shows the assessment of liquefaction potential ("triggering") at the location of each individual SPT. All of the SPT blowcounts are shown versus depth in the lower left plot. The upper right plot places the SPT blowcounts for the soils found likely to liquefy within the potential shear strain curves of Wu (2002). The accumulation of the resulting potential shear strain, summed vertically over the boring and converted to Displacement Potential Index, *DPI*, for each sub-layer is illustrated in the lower right plot. Also shown in the lower right plot is the maximum, mean and mean ± one standard deviation measured horizontal displacement for comparison to *DPI*.

O' Rourke et al (1992) estimated horizontal displacements and vertical settlements by analyzing photographs taken of the area after the earthquake. These measurements were separated into zones of similar movement (Zone A and B). This case consists of the soil mass is identified as Zone B, which experienced a maximum displacement of 2.1m. Cultural features were used to measure displacements, such as curbs or railroad rails, which results in a highly uncertain measurement. The ground slope is an average of that presented in O'Rourke et al. (1992), resulting in an α of 1.5%.

The estimate of maximum lateral spread displacement using Eq. 2 for the Mission Creek case history is 3.3m. This falls within a factor of two of the maximum measured lateral spread displacement of 2.1m, reasonable accuracy given the age of the case history and hence quality of data upon which the estimate is based.

Conclusions

The maximum displacement was chosen to represent the magnitude of liquefaction-induced lateral spread displacement for two main reasons: usability in a forward sense and data availability. First, an engineer concerned with performance wants to know the maximum displacement expected to occur at a site for the design scenario earthquake. Second, post-earthquake reconnaissance investigators are attracted to the highest level of damage and so the documented displacements are often the largest observed. The approach taken in this work to model the maximum displacement is based on knowledge gained from both laboratory testing and field case histories, represented by the maximum displacement potential index, DPI_{max} and so represents a "semi-empirical" approach. The recommended semi-empirical model was regressed using Bayesian updating methods to develop a correlation between DPI_{max} and the maximum observed lateral displacement of a given lateral spread feature. Additional variables included in the correlation were static "driving" shear stresses and magnitude of the causative earthquake (which served as a proxy for duration, or number of cycles of shaking). The resulting correlation produced a good overall prediction of the cases studied, with a predictive capability generally within a factor of two of the observed maximum displacements, as illustrated in the Mission Creek case history.

References

Abrahamson, N.A. and W.J. Silva, 1997. Empirical Response Spectral Attenuation Relations for Shallow Crustal Earthquakes, *Seismological Research Letters* 68 (1), 94-127.

Bartlett, S.F., 1992. Empirical Analysis of Horizontal Ground Displacement Generated By Liquefaction-Induced Lateral Spreads, *Ph. D. Dissertation*, Brigham Young University.

Cetin, K.O., 2000. Reliability-Based Assessment of Seismic Soil Liquefaction Initiation Hazard, *Ph. D. Dissertation*, University of California, Berkeley.

Dickenson, S.E., 1994. Dynamic Response of Soft and Deep Cohesive Soils During the Loma Prieta Earthquake of October 17, 1989, *Ph. D. Dissertation*, University of California, Berkeley.

O' Rourke, T.D., P.A. Beaujon, and C.A. Scawthorn, 1992. Large Ground Deformation and Their Effects on Lifeline Facilities: 1906 San Francisco Earthquake, *Case Studies of Liquefaction and Lifeline Performance During Past Earthquakes*, NCEER-92-0002, National Center for Earthquake Engineering Research, Buffalo, N.Y.

Sadigh, R.K. and J. A. Egan, 1998. Updated Relationships for Horizontal Peak Ground Velocity and Peak Ground Displacement for Shallow Crustal Earthquakes, *Sixth U.S. National Conference on Earthquake Engineering*, Earthquake Engineering Research Institute.

Seed, H.B., K. Tokimatsu, L.F. Harder, and R.M. Chung, 1985. Influence of SPT Procedures in Soil Liquefaction Resistance Evaluations, *Journal of the Geotechnical Engineering*, 111 (12), 1425-1455.

Seed, R.B., K.O. Cetin, R.E.S. Moss, A.M. Kammerer, J. Wu, J.M. Pestana, and M.F. Riemer, 2001. Recent Advances in Soil Liquefaction Engineering and Seismic Site Response Evaluation, *Proceedings: Fourth International Conference on Recent Advances in Geotechnical Earthquake Engineering and Soil Dynamics*, Paper No. SPL-2.

Sykora, D.W. and K.H. Stokoe, 1983. Correlations of In-situ Measurements in Sands with Shear Wave Velocity, *Geotechnical Engineering Report GR 83-33*, University of Texas, Austin.

Wu, J., 2002. Liquefaction Triggering and Post Liquefaction Deformations of Monterey 0/30 Sand under Uni-Directional Cyclic Simple Shear Loading. *Ph. D. Dissertation*, University of California, Berkeley.

Youd, T.L., I.M. Idriss, R.D. Andrus, I. Arango, G. Castro, J.T. Christian, R. Dobry, W.D.L. Finn, L.F. Harder, M.E. Hynes, K. Ishihara, J.P. Koester, S.C. Liao, W.F. Marcuson, G.R. Martin, J.K. Mitchell, Y. Moriwaki, M.S. Power, P.K. Robertson, R.B. Seed, and K.H. Stokoe, 2001. Liquefaction Resistance of Soils: Summary Report from the 1996 NCEER/NSF Workshops on Evaluation of Liquefaction Resistance of Soils, *Journal of the Geotechnical and Geoenvironmental Engineering*, 127 (410), 817-833.